

Flowing Crystals: Non-Equilibrium Structure of Foam

Piotr Garstecki^{1,2} & George M. Whitesides¹

¹ *Department of Chemistry and Chemical Biology, Harvard University,*

12 Oxford St., Cambridge, MA, U.S.A.

² *Institute of Physical Chemistry, Polish Academy of Sciences,*

Kasprzaka 44/52, 01-224 Warsaw, Poland

Supplemental Material

1. An additional example of the bubble lattices (obtained for $d/w = 0.66$).

In Supplemental Figure 1 we show an additional example of lattices of bubbles formed in a system in which the width of the outlet channel $w = 250 \mu\text{m}$. In this system, and for the bubbles of equivalent diameter $d = (4A/\pi)^{1/2} = 165 \mu\text{m}$, where A is the surface area of the top interface of the bubble, we observed generation of only two types of lattices – *hex-one* and *hex-two*. The second of these lattices (*hex-two*) has a lower total perimeter of the bubbles and thus lower interfacial energy. At low pressures applied to the system we observe chiefly generation of the *hex-two* lattice, while at high pressures the ‘occupation’ of states inverts and we observe predominantly formation of the *hex-one* lattice.

2. Image analysis.

We used home-made image analysis software that loads the avi video files and analyzes the frames. The analysis of each frame of the video is conducted as follows. First,

we choose a region in the (n -th) frame that exhibits the outlet channel, and we threshold this region to obtain a matrix $M_n(x,y)$ that acquires values of zero or one (corresponding to either ‘no-signal’ for pixels representing gas or the ‘signal’ for pixels representing the interface between bubbles) for each pixel (x,y) inside the channel (x is the coordinate along the length of the channel and y is the coordinate along its width). Second we calculate a border distribution $I_n(y) = \sum M_n(x,y)$, where the sum runs over all x 's. Next we manually inspect a number (typically ~ 20) of frames and assign the labels (names of the structures, including ‘disordered’ as one of the types) to them. We store the distributions I_i for these frames as ‘masters’ and compare all the other frames to them. Numerically, we compare two distributions n and i by calculating the sum D_{ni} of the squares of the differences between the values of these distributions at any particular value of y : $D_{ni} = \sum (I_n(y) - I_i(y))^2$, where the sum runs over all y 's. In this way the routine assigns to each frame n a label of frame i for which D_{ni} is smallest. We then review a sample set of (typically 20 to 50) labels assigned by the program and if a frame was assigned a wrong label, we list this frame as an additional ‘master’ with a correct label. We then iterate the steps of automatic recognition and ‘teaching’ of the program until we do not find any frames that are mislabeled. For each new movie that we analyze using a ‘thought’ program, we check the labels assigned automatically and we correct errors. We found that this procedure can successfully discriminate between the structures – after few ‘learning’ steps we did not find any incorrectly assigned labels.

3. Stability of the bubble lattices.

In Supplemental Figure 2a we show the result of the automatic recognition of the structure of the lattice of bubbles. As we described in the Letter, the system switches between formation of different lattices. The transition from generation of one type of an

ordered structure to another usually proceeds through a short interval during which the system produces a disordered array of bubbles. Although these ‘switching’ events do not seem to follow any regular pattern, an inspection of the histogram of the counts of frames exhibiting disordered arrays (see Fig. 2b) suggests, that the appearance of slightly longer intervals during which disordered arrays are produced occurs at regular intervals. This observation, together with an observation that the ‘characteristic interval’ between patches of disordered arrays decreases with increasing rate of flow of the fluids through the system, suggested that the origin – of at least part – of the switching events could lay in the fluctuations of pressure applied to the stream of the liquid by the syringe pump.

In order to verify this assertion we conducted experiments without the syringe pump. In these experiments both the liquid and the gas phase were drawn from a pressurized container. In addition, in order to control the relative rate of flow of the two phases, we used an adjustable clamp on the tubing delivering the liquid from the pressurized tank to the microfluidic device (Figure 3). (A variation of this setup included two independently pressurized tanks – one for the gas phase and one for the liquid. We found, however, that it was difficult to stabilize the system in this arrangement). We found that for any pressure p applied to the pressurized container we can adjust the rate of flow of the liquid (by tuning the clamp) to a value which resulted in formation of bubbles with equivalent diameters similar to those inspected in the experiments with the syringe pump, and at high volume fractions ($\phi \approx 1$). In agreement with our expectations, the system was switching between different structures less often than in the experiments with the use of a syringe pump. Figure 4 shows an example of a prolonged formation of one type of the lattice (*hex-three*) for sixty seconds, with only one short period during which a disordered lattice was produced. In this example the fluctuation was caused by an event of coalescence of two bubbles in the channel.

We found it, nonetheless, difficult to obtain a series of the fractions P_i during which the system produces any type of lattice over a wide range of pressures. The reason for this difficulty laid in the that the bubbles were formed at high volume fraction only at high values of the ratio of the rates of flow of gas to the rate of flow of liquid, and very close to ratios at which the stream of gas was no longer breaking in the orifice. Figure 5 illustrates two structures formed at $p = 94$ kPa and an array of bubbles during the transition, together with a micrograph of the system when the stream of gas did not break in the orifice.

Captions for Supplemental Figures

Supplemental Figure 1. In insets a and b we show the micrographs of two structures that we observed for the ratio of the equivalent diameter of the bubbles ($d = 165 \mu\text{m}$) to the width of the channel ($w = 250 \mu\text{m}$) equal to $d/w = 0.66$. The height of the channel used in this experiment was $h = 25 \mu\text{m}$, the pressure applied to the stream of gas was $p = 138.8 \text{ kPa}$, and the rate of flow of the aqueous solution was $Q = 0.55 \mu\text{L/s}$. Inset c shows the fractions of time that the system produced the two phases for a range of pressures applied to the stream of gas $p \in (70, 189) \text{ kPa}$. The open circles represent the fraction of time during which the system produced the *hex-one* lattice (shown in inset a), and the filled circles show the fractions of time during which the system produced the *hex-two* lattice (inset b). The solid lines are drawn to guide the eye only.

Supplemental Figure 2. a) A graph showing the structure produced by the system discussed in our letter ($w = 750 \mu\text{m}$, $h = 25 \mu\text{m}$, $p = 104 \text{ kPa}$, $Q = 0.46 \mu\text{L/s}$) as a function of time. There are 5000 data points corresponding to the 5000 frames that we captured at 10 ms intervals. b) a histogram of the number of frames showing disordered arrays of bubbles per 100 ms intervals. The thick lines suggest possible regular component in the appearance of the disordered lattices and thus in the fluctuations in pressures applied to the system.

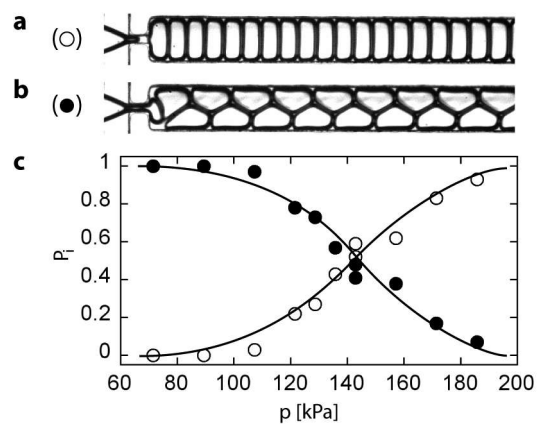
Supplemental Figure 3. A schematic diagram of the experimental setup that we used to decrease the fluctuations of the pressure applied to the inlets supplying the aqueous phase to the microfluidic device. The setup comprised a sealed container half-filled with the aqueous solution and three tubes. One of the tubes delivered nitrogen from a pressurized tank, at an externally controlled pressure p . The two other tubes (one contacting the liquid, the other gas) delivered the two immiscible phases to the microfluidic device. We controlled the ratio

of the rates of flow of the gaseous and liquid phases by adjusting the a clamp on the tubing that delivered liquid to microfluidic device.

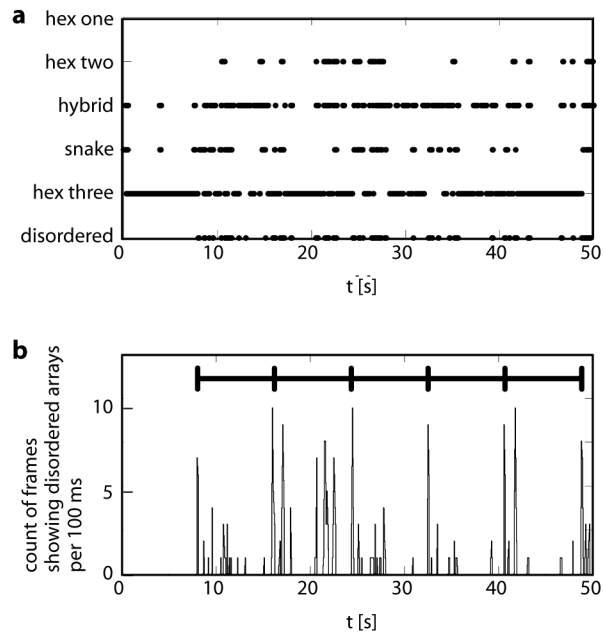
Supplemental Figure 4. a) Graph showing the type of the lattice formed by a system operated with pressurized inlets as a function of time ($w = 750 \mu\text{m}$, $h = 25 \mu\text{m}$, $p = 20 \text{kPa}$). Please note that generation of the *hex-three* lattice is interrupted by a short interval during which a ‘disordered array’ of bubbles was produced at $t \approx 47.88 \text{ s}$. Inset b) shows a close-up on the time-series presented in a). In insets c and d we show micrographs of the lattices produced just before the fluctuation (an event of coalescence of two bubbles), and right after, respectively.

Supplemental Figure 5. a) Graph illustrating the type of the lattice generated by the system ($w = 750 \mu\text{m}$, $h = 25 \mu\text{m}$, $p = 94 \text{kPa}$) as a function of time. We recorded the movie at a rate of ten thousand frames per second. The system switches from generation of the *snakeskin* lattice (shown in inset b) to formation of the *hex-two* lattice (inset d) and a short transient array of bubbles can be seen (inset c) during this switching. In inset e we show a micrograph of the system when the stream of gas does not break at the orifice ($p = 94 \text{kPa}$).

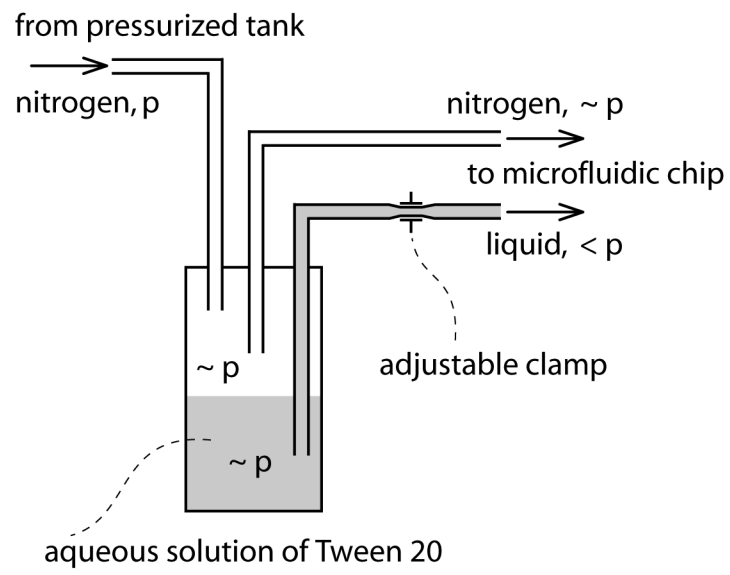
Supplemental Figures



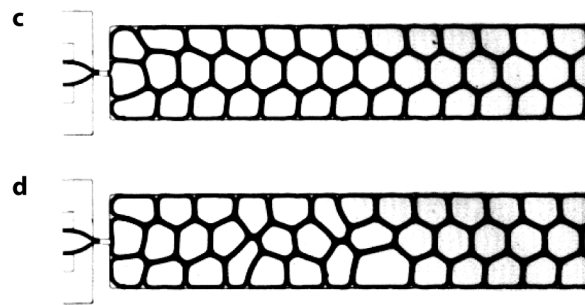
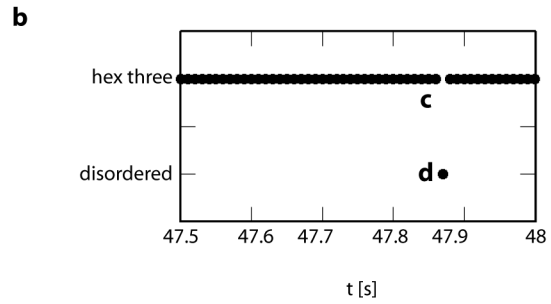
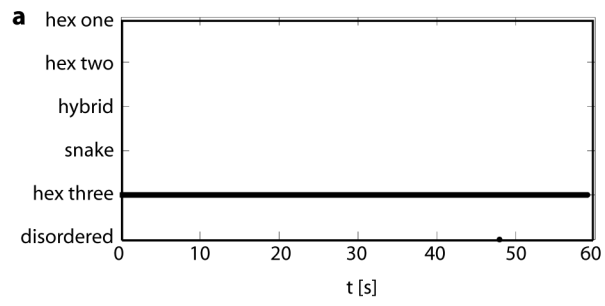
Supplemental Figure 1.



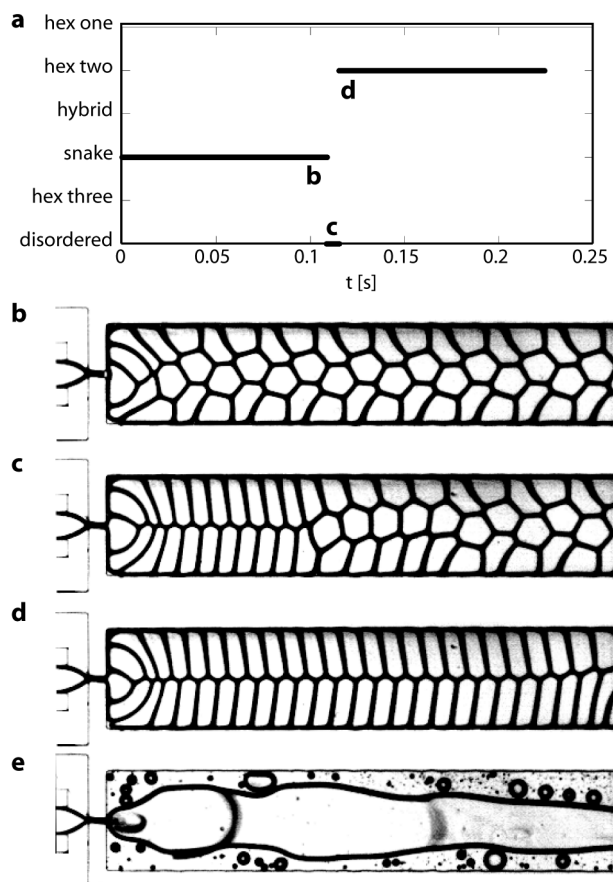
Supplemental Figure 2.



Supplemental Figure 3.



Supplemental Figure 4.



Supplemental Figure 5.